

**Strong anisotropy in the electromagnetic properties of  $\text{Na}_2\text{Ti}_2\text{X}_2\text{O}$  ( $X = \text{As}, \text{Sb}$ ) crystals**

Y. G. Shi, H. P. Wang, X. Zhang, W. D. Wang, Y. Huang, and N. L. Wang

*Beijing National Laboratory for Condensed Matter Physics, Institute of Physics, Chinese Academy of Sciences, Beijing 100190, China*

(Received 14 July 2013; revised manuscript received 3 October 2013; published 24 October 2013)

$\text{Na}_2\text{Ti}_2\text{X}_2\text{O}$  ( $X = \text{As}, \text{Sb}$ ) crystals have been grown from the flux method. X-ray diffraction characterization revealed an anti- $\text{K}_2\text{NiF}_4$ -type layered structure (tetragonal, space group  $I4/mmm$ ) for both compounds. Magnetic susceptibility ( $\chi(T)$ ) and electrical resistivity ( $\rho(T)$ ) measurements revealed major kinks at  $\sim 115$  K ( $T_{s1}$ ) and  $\sim 320$  K ( $T_{s2}$ ) for  $\text{Na}_2\text{Ti}_2\text{Sb}_2\text{O}$  and  $\text{Na}_2\text{Ti}_2\text{As}_2\text{O}$ , respectively, signifying possibly the opening of density wave gaps. Both  $\text{Na}_2\text{Ti}_2\text{Sb}_2\text{O}$  and  $\text{Na}_2\text{Ti}_2\text{As}_2\text{O}$  showed remarkably strong anisotropy in their electromagnetic transport properties, and values of  $\gamma_\rho$  ( $\rho_c/\rho_{ab}$ ) even reached  $\sim 140$  and  $\sim 430$ , respectively, being much larger than that of iron pnictide  $\text{BaFe}_2\text{As}_2$  ( $\gamma_\rho \sim 2-5$ ). The  $\gamma_\rho$  of  $\text{Na}_2\text{Ti}_2\text{Sb}_2\text{O}$  changed slightly with cooling, though a small drop at  $T_{s1}$  occurred. In contrast, the  $\gamma_\rho$  of  $\text{Na}_2\text{Ti}_2\text{As}_2\text{O}$  changed strikingly by exhibiting not only a small change at  $T_{s2}$  but also a sudden decrease of  $\sim 50$  K, reduced nearly 1/3. Specific heat measurement indicated that  $\text{Na}_2\text{Ti}_2\text{Sb}_2\text{O}$  was only partially gapped with  $\gamma_1 = 4.1$  mJ mol $^{-1}$  K $^{-2}$ , though a long-range order was established at  $T_{s1}$ , while  $\text{Na}_2\text{Ti}_2\text{As}_2\text{O}$  was fully gapped. The remarkably strong electromagnetic anisotropy revealed in  $\text{Na}_2\text{Ti}_2\text{X}_2\text{O}$  suggests the crucial role of the  $\text{TiO}_2\text{X}_4$  layer for the transport properties of layered titanium oxypnictides.

DOI: [10.1103/PhysRevB.88.144513](https://doi.org/10.1103/PhysRevB.88.144513)

PACS number(s): 74.70.Xa, 72.15.-v, 74.25.F-, 75.30.Gw

**I. INTRODUCTION**

To date, high- $T_c$  superconductivity only appears in layered materials such as cuprates and iron arsenides, in which the strongly correlated electrons in two-dimensional (2D) electron system dominate the transport properties and hence lead to a notable feature of strong electronic anisotropy. Electronic anisotropy imposed in the layered structure can reach a remarkably high degree, with the out-of-plane  $c$ -axis resistivity  $\rho_c(T)$  being orders of magnitude larger than in-plane resistivity  $\rho_{ab}(T)$  in the normal state.<sup>1,2</sup> Superconductivity can even survive in cuprates when the 2D  $\text{CuO}_2$  plane is essentially decoupled,<sup>3-6</sup> thus suggestive of a pivotal role of the 2D  $\text{CuO}_2$  layer in giving rise to high- $T_c$  superconductivity. Furthermore, unconventional superconductivity, including particularly high- $T_c$  superconductivity, usually appears neighboring other orders of ground states, like charge-density wave (CDW),<sup>7,8</sup> spin-density wave (SDW),<sup>9,10</sup> or magnetism (anti- or ferromagnetism).<sup>11</sup> The presence of competing phenomena also offers important clues for understanding the superconductivity. The superconductivity in iron arsenides in proximity to magnetism, for instance, has been widely believed to gain energy from the spin fluctuations to have a high  $T_c$ .<sup>12-14</sup> Thus, a system with both features of a 2D electron system imposed in a layered structure and SDW, CDW, or magnetism would be of interest in serving as an excellent platform for exploration of unusual superconductivity. In this regard, layered titanium oxypnictides with the formula  $Ln\text{Ti}_2\text{X}_2\text{O}$  ( $Ln = \text{Ba}, \text{Na}_2, (\text{SrF})_2, (\text{SmO})_2$ ;  $X = \text{As}, \text{Sb}$ ) naturally deserve more attention, because they are promising in regard to meeting both requirements.<sup>15-24</sup> Recently, superconductivity with a  $T_c$  of  $\sim 1.2$  K was discovered in  $\text{BaTi}_2\text{Sb}_2\text{O}$ .<sup>21</sup> The superconductivity appears after a precursory phase transition at  $\sim 50$  K. However, conclusions on the nature of the phase transition and its correlation with the superconductivity have not come to a consensus. Associated with the magnetic susceptibility and resistivity anomalies, a structural distortion in the  $\text{Ti}_2\text{Sb}_2\text{O}$  layer, rather than long-range magnetic ordering, was detected by a very early powder neutron diffraction

measurement on  $\text{Na}_2\text{Ti}_2\text{Sb}_2\text{O}$ .<sup>25</sup> Density functional theory (DFT) calculations indicated a density wave (DW) instability due to the nesting of the nearly 2D Fermi surface.<sup>16</sup> Recently, the arguments have been converged to the types of DW states, i.e., CDW or SDW.<sup>26</sup> Subedi performed DFT calculations on  $\text{BaTi}_2\text{Sb}_2\text{O}$ , and the results suggested a CDW instability.<sup>27</sup> Being consistent with this calculation, a nuclear magnetic resonance and nuclear quadrupole resonance measurements on  $\text{BaTi}_2\text{Sb}_2\text{O}$  did not reveal any signature of magnetic order at low temperature and indicated a possible commensurate CDW ordering.<sup>28</sup> However, more recent DFT calculations on  $\text{Na}_2\text{Ti}_2\text{X}_2\text{O}$  indicated SDW instabilities.<sup>29-31</sup>

$\text{Na}_2\text{Ti}_2\text{Sb}_2\text{O}$  and  $\text{Na}_2\text{Ti}_2\text{As}_2\text{O}$  exhibit phase transitions at different temperatures. For  $\text{Na}_2\text{Ti}_2\text{Sb}_2\text{O}$  it is  $\sim 115$  K ( $T_{s1}$ ),<sup>18,25</sup> while for  $\text{Na}_2\text{Ti}_2\text{As}_2\text{O}$  it takes place at a much higher temperature of  $\sim 320$  K ( $T_{s2}$ ).<sup>15,18</sup>  $\text{Na}_2\text{Ti}_2\text{X}_2\text{O}$  has a similar structure as that of  $\text{La}_2\text{CuO}_4$ , which crystallizes in a  $\text{K}_2\text{NiF}_4$ -type layered structure,<sup>11</sup> but the  $\text{Ti}_2\text{O}$  square lattice, formed by edge-shared  $\text{TiO}_2\text{X}_4$  octahedra, with  $\text{Ti}^{3+}(3d^1)$  being coordinated by two oxide anions and four pnictide anions, adopts an anticonfiguration to the  $\text{CuO}_2$  square lattice in  $\text{LaCu}_2\text{O}_4$ .<sup>25</sup> In this anti- $\text{K}_2\text{NiF}_4$ -type layered structure (space group  $I4/mmm$ ), the edge-shared  $\text{TiO}_2\text{X}_4$  octahedra are alternatively stacked and interspersed by double  $\text{Na}^+$  layers along the  $c$  axis. In the electronic structure of  $\text{Na}_2\text{Ti}_2\text{X}_2\text{O}$ , the Ti  $3d$  orbitals, being hybridized with the  $X p$  orbitals in the layer, are mainly involved in the multiband structure at the Fermi level, and the  $\text{TiO}_2\text{X}_4$  layers are believed to dominate the transport properties;<sup>27</sup> thus, an electronic anisotropy would be expected. Considering the many similarities between  $\text{Na}_2\text{Ti}_2\text{X}_2\text{O}$  and iron-based superconductors, study on electronic anisotropy of them would be helpful for further understanding the role of the 2D electron system for the transport properties. Moreover, aiming at unveiling the nature of the phase transition in  $\text{Na}_2\text{Ti}_2\text{X}_2\text{O}$ , electromagnetic data on a single crystal are also desirable. Though crystal growth of  $\text{NaTi}_2\text{Sb}_2\text{O}$  was already reported,<sup>25</sup> detailed electromagnetic characterizations have so far been absent. We have

systematically investigated  $\text{Na}_2\text{Ti}_2\text{Sb}_2\text{O}$  and  $\text{Na}_2\text{Ti}_2\text{As}_2\text{O}$  single crystals by means of x-ray diffraction (XRD), magnetic susceptibility, isothermal magnetization, electrical resistivity, and specific heat measurements. Electromagnetic anisotropy of the crystals is our primary focus.

## II. EXPERIMENTAL DETAILS

$\text{Na}_2\text{Ti}_2\text{As}_2\text{O}$  and  $\text{Na}_2\text{Ti}_2\text{Sb}_2\text{O}$  single crystals were grown using the flux method. NaAs and NaSb flux were prepared beforehand by separately reacting the stoichiometric mixture of the Na (2N) chunk and the As (4N) or Sb (4N) powder in evacuated and sealed quartz tubes. Mixture of Na and As was slowly heated to  $400^\circ\text{C}$ , while Na and Sb was heated to  $350^\circ\text{C}$ , and both were reacted at the temperatures for 12 h. High-purity starting materials of Ti (4N) and  $\text{TiO}_2$  powder (5N) were mixed together with flux in a molar ratio of 3:1:20. They were put into  $\text{Al}_2\text{O}_3$  ampoules, and the assembly was sealed into Ta tubes under argon gas. The Ta tubes were then sealed in evacuated quartz tubes and afterward heated in a furnace. For  $\text{Na}_2\text{Ti}_2\text{As}_2\text{O}$ , the reaction was at  $1050^\circ\text{C}$  for 5 h, followed by a slow cooling to  $750^\circ\text{C}$  at a rate of  $3^\circ\text{C}/\text{h}$ . For  $\text{Na}_2\text{Ti}_2\text{Sb}_2\text{O}$ , the reaction was at  $1120^\circ\text{C}$  for 5 h; it was cooled to  $820^\circ\text{C}$  at a rate of  $3^\circ\text{C}/\text{h}$ . Both tubes were then cooled quickly to  $600^\circ\text{C}$ , following the slow cooling process, and inverted and spun immediately in a centrifugal separator at this temperature to remove excess flux. After separating the flux, platelike single crystals with a typical dimension of  $\sim 3 \times 3 \times 0.1 \text{ mm}^3$  were left.

Phase identification of the crystals was performed at room temperature on a Shimadzu XRD-7000 x-ray diffractometer using  $\text{Cu K}\alpha 1$  ( $\lambda = 1.540596 \text{ \AA}$ ). XRD data were collected in a  $2\theta$  range of  $5\text{--}80^\circ$  with a scan step interval of  $0.02^\circ$ . The anisotropic resistivity was measured using a generalization of the Montgomery method.<sup>32</sup> The typical dimensions of crystals used to determine the resistivity were  $\sim 1.2 \times 1.0 \times 0.07 \text{ mm}^3$  for  $\text{Na}_2\text{Ti}_2\text{Sb}_2\text{O}$  and  $1.7 \times 1.8 \times 0.06 \text{ mm}^3$  for  $\text{Na}_2\text{Ti}_2\text{As}_2\text{O}$ , with the shortest being the lattice constant  $c$ . The measurement was conducted by cooling samples in a physical properties measurement system from Quantum Design (QD). Magnetic susceptibility ( $\chi$ ) for both the  $H\parallel ab$  plane and the  $H\parallel c$  axis was measured between 2 and 400 K under zero-field-cooling (ZFC) and field-cooling (FC) conditions in a superconducting quantum interference device–vibrating sample magnetometer from QD. A magnetic field ( $H$ ) of 50 kOe was employed. Specific heat ( $C_p$ ) was measured on the same apparatus by a time-relaxation method between 2 and 300 K. About 3.6-mg crystals of  $\text{Na}_2\text{Ti}_2\text{Sb}_2\text{O}$  and 2.0 mg of  $\text{Na}_2\text{Ti}_2\text{As}_2\text{O}$  were selected for use.

## III. RESULTS AND DISCUSSION

Typical single-crystal XRD patterns for  $\text{Na}_2\text{Ti}_2\text{As}_2\text{O}$  and  $\text{Na}_2\text{Ti}_2\text{Sb}_2\text{O}$  are presented in Fig. 1. A preferred orientation toward  $[0\ 0\ 2n]$  ( $n$  is an integer) is observed, though very small peaks probably arising from other orientations or some unidentified impurities are also detected. This indicates that the  $c$  axis of the crystals synthesized in this paper is basically perpendicular to the crystal plane ( $ab$  plane). In addition, the good formation of the expected tetragonal

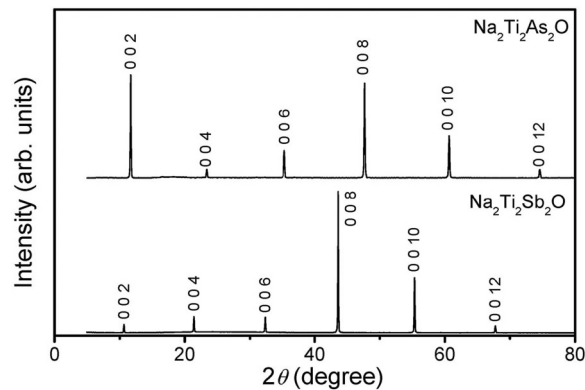


FIG. 1. Room temperature XRD patterns of the  $\text{Na}_2\text{Ti}_2\text{X}_2\text{O}$  ( $X = \text{As}, \text{Sb}$ ) crystals with the main Bragg reflection being indexed, showing main  $c$ -axis orientation with very sharp peaks.

crystal structure (space group  $I4/mmm$ ) was confirmed by indexing the peaks using the tetragonal primitive unit cell. The calculated lattice constant for  $\text{Na}_2\text{Ti}_2\text{As}_2\text{O}$  is  $c = 15.2835 \text{ \AA}$ , and for  $\text{Na}_2\text{Ti}_2\text{Sb}_2\text{O}$ , it is  $c = 16.5847 \text{ \AA}$ ; these are roughly consistent with the values reported previously.<sup>18,20</sup> The XRD characterization thus suggests the reliability of the crystal quality.

The  $\chi(T)$  measured for  $H\parallel c$  ( $\chi_c$ ) and  $H\parallel ab$  ( $\chi_{ab}$ ) of  $\text{Na}_2\text{Ti}_2\text{Sb}_2\text{O}$  and  $\text{Na}_2\text{Ti}_2\text{As}_2\text{O}$  crystals, respectively, are depicted separately in Figs. 2(a) and 3(a). Even at a first glance, common features between the two compounds are strikingly displayed. First,  $\chi_c$  is much larger than  $\chi_{ab}$ . Second, the ZFC and FC data in both directions show no difference within measured temperature range.

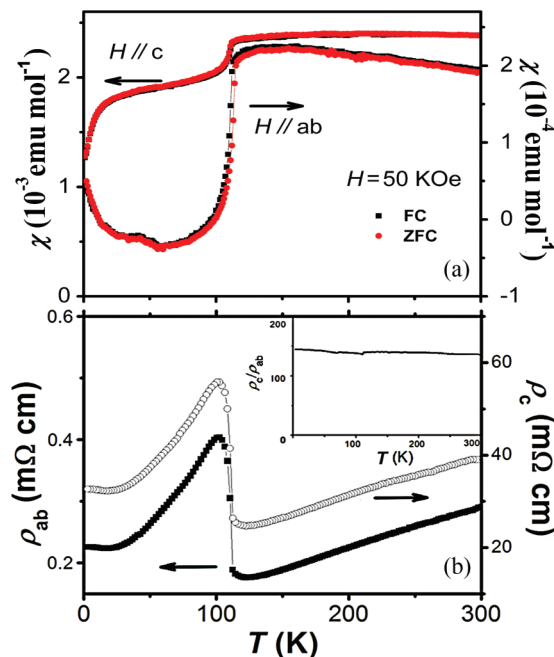


FIG. 2. (Color online) (a) The magnetic susceptibility  $\chi$  vs  $T$  of  $\text{Na}_2\text{Ti}_2\text{Sb}_2\text{O}$  measured for  $H\parallel c$  ( $\chi_c$ ) and  $H\parallel ab$  ( $\chi_{ab}$ ) in 50 kOe. (b) The anisotropic resistivity  $\rho$  vs temperature  $T$  measured on a single crystal in a zero magnetic field.

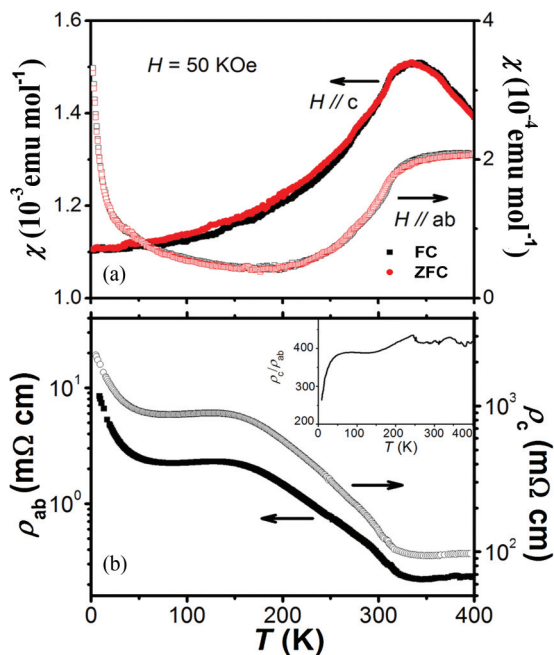


FIG. 3. (Color online) (a) The anisotropic magnetic susceptibility  $\chi$  vs  $T$  of  $\text{Na}_2\text{Ti}_2\text{As}_2\text{O}$  measured in 50 kOe. (b) The anisotropic electrical resistivity  $\rho$  vs temperature  $T$  measured in a zero magnetic field.

Third, sudden drops of  $\chi(T)$  for  $\text{Na}_2\text{Ti}_2\text{Sb}_2\text{O}$  and  $\text{Na}_2\text{Ti}_2\text{As}_2\text{O}$  in both directions starting at  $T_{s1}$  ( $\sim 115$  K) and  $T_{s2}$  ( $\sim 320$  K) are strikingly displayed, being in agreement to previously reported phase transition temperatures for them. The drop of  $\chi_{ab}$  for  $\text{Na}_2\text{Ti}_2\text{Sb}_2\text{O}$  is apparently much sharper than that for  $\text{Na}_2\text{Ti}_2\text{As}_2\text{O}$ . Moreover,  $\chi_c$  of the two crystals decreases monotonically below  $T_{s1}$  and  $T_{s2}$ , while  $\chi_{ab}$  first shows a decrease to a local minimum of  $\sim 60$  and  $\sim 150$  K for  $\text{Na}_2\text{Ti}_2\text{Sb}_2\text{O}$  and  $\text{Na}_2\text{Ti}_2\text{As}_2\text{O}$ , respectively, and then starts to rise. The rise became steep at  $\sim 20$  and  $\sim 60$  K for  $\text{Na}_2\text{Ti}_2\text{Sb}_2\text{O}$  and  $\text{Na}_2\text{Ti}_2\text{As}_2\text{O}$ , respectively, with Curie-Weiss-like tails on  $\chi_{ab}$  at low temperature. The evaluated effective moments for

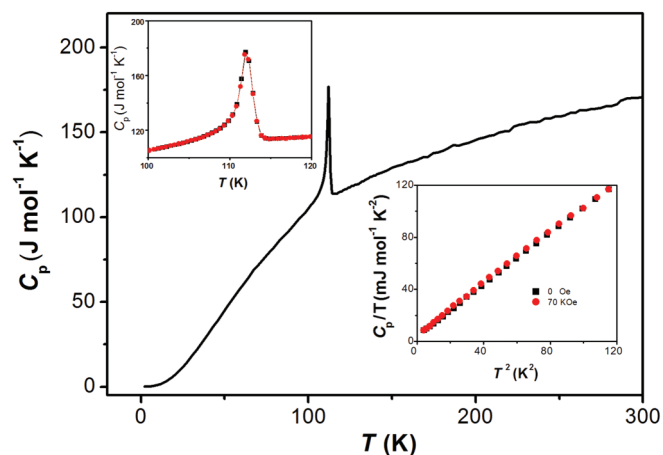


FIG. 4. (Color online) Temperature-dependent heat capacity  $C_p$  of  $\text{Na}_2\text{Ti}_2\text{Sb}_2\text{O}$ . The upper left inset indicates an expansion of the data in the vicinity of the peak. The lower right inset indicates the lowest temperature limit of the data in the plot of  $C_p/T$  vs  $T^2$ .

the tails are  $\sim 0.04 \mu_B/\text{f.u.}$  and  $0.17 \mu_B/\text{f.u.}$  for  $\text{Na}_2\text{Ti}_2\text{Sb}_2\text{O}$  and  $\text{Na}_2\text{Ti}_2\text{As}_2\text{O}$ , respectively.

Finally, in the overall profiles of  $\chi(T)$  for both  $\text{Na}_2\text{Ti}_2\text{Sb}_2\text{O}$  and  $\text{Na}_2\text{Ti}_2\text{As}_2\text{O}$ , magnetic anisotropies with respect to the two directions of  $H\parallel ab$  and  $H\parallel c$  are apparently gradually weakened below  $T_{s1}$  and  $T_{s2}$ , thus indicating a close relation between the DW-type gap formation and the magnetic anisotropy.

The main panels of Figs. 2(b) and 3(b) present the temperature dependence of resistivity  $\rho(T)$  for  $\text{Na}_2\text{Ti}_2\text{Sb}_2\text{O}$  and  $\text{Na}_2\text{Ti}_2\text{As}_2\text{O}$ , respectively, measured for two resistivity components  $\rho_c$  and  $\rho_{ab}$  on a single sample. The common features between them are as follows: (1)  $\rho_c$  and  $\rho_{ab}$  have a similar profile, (2)  $\rho_c$  is much larger than  $\rho_{ab}$  over the measured temperature range, and (3) clear metal-insulator transitions (MITs) at  $T_{s1}$  and  $T_{s2}$  for  $\text{Na}_2\text{Ti}_2\text{Sb}_2\text{O}$  and  $\text{Na}_2\text{Ti}_2\text{As}_2\text{O}$  are visible. Nevertheless, some differences are also clearly exhibited. First, for  $\text{Na}_2\text{Ti}_2\text{Sb}_2\text{O}$ , after the very sharp MIT at  $T_{s1}$ , an insulator-metal transition appears at nearly the same temperature at  $T_{s1}$  on both  $\rho_c$  and  $\rho_{ab}$ , and the metallic conduction then shows slight upturns below  $\sim 20$  K. The slight upturn is possibly induced by a weak electron localization effect. For  $\text{Na}_2\text{Ti}_2\text{As}_2\text{O}$ , two shoulderlike features appear on both  $\rho_c$  and  $\rho_{ab}$ . The first part is between  $T_{s2}$  and 400 K before the MIT due to a poorly metallic conduction, and the second part is between  $\sim 60$  and  $\sim 150$  K due to a poorly insulating conduction. Below  $\sim 50$  K, the upturns of both  $\rho_c$  and  $\rho_{ab}$  are more prominent than those observed for  $\text{Na}_2\text{Ti}_2\text{Sb}_2\text{O}$ . These characterized temperatures for  $\rho(T)$  coincide well with those derived from  $\chi(T)$ , indicating an intimate relationship between magnetic and electronic correlations. In contrast to  $\text{Na}_2\text{Ti}_2\text{Sb}_2\text{O}$  being primarily metallic except for the very weak low-temperature upturn,  $\text{Na}_2\text{Ti}_2\text{As}_2\text{O}$  remains insulating after the MIT.

Second, seen from the plotted  $\rho_c/\rho_{ab}$  ( $\gamma_\rho$ ) ratio as a function of temperature by the inset in Fig. 3(a) for  $\text{Na}_2\text{Ti}_2\text{Sb}_2\text{O}$ , a slightly drop of  $\gamma_\rho$  that occurred at  $\sim 115$  K could be observed, from  $\sim 140$  to  $\sim 135$ ;  $\gamma_\rho$  then increases slightly with cooling. The values of  $\gamma_\rho$  for  $\text{Na}_2\text{Ti}_2\text{Sb}_2\text{O}$  are quite large compared with the typical value for iron pnictides,  $\sim 2$ – $5$  for  $\text{BaFe}_2\text{As}_2$ , indicating a highly anisotropic electronic nature of  $\text{Na}_2\text{Ti}_2\text{Sb}_2\text{O}$ . For  $\text{Na}_2\text{Ti}_2\text{As}_2\text{O}$ ,  $\gamma_\rho$  is higher than 400 above 300 K, indicative of a remarkably anisotropic electronic structure. A rapid drop below 50 K from  $\sim 380$  at 50 K to  $\sim 264$  at 2 K, rather than at  $T_{s2}$ , is strikingly displayed, and the change at  $T_{s2}$  is hard to identify due to the data quality. Nevertheless, the  $\gamma_\rho$  values are remarkably larger than those of  $\text{Na}_2\text{Ti}_2\text{Sb}_2\text{O}$ . The sharp drop of  $\gamma_\rho$  below 50 K for  $\text{Na}_2\text{Ti}_2\text{As}_2\text{O}$  implies that the band structure is reconstructed again. It seems that the compound experiences another phase transition below 50 K. Subtle features seem to be present in the magnetization and specific heat measurement near 40 K, but this issue needs further exploration.

Figures 4 and 5 show the specific heat data of  $\text{Na}_2\text{Ti}_2\text{Sb}_2\text{O}$  and  $\text{Na}_2\text{Ti}_2\text{As}_2\text{O}$ , respectively. For  $\text{Na}_2\text{Ti}_2\text{Sb}_2\text{O}$ , a lambda-like kink at  $T_{s1}$  with a sharp peak is visible, indicating the establishment of a long-range order due to the DW-type gap opening. For  $\text{Na}_2\text{Ti}_2\text{As}_2\text{O}$ , we failed to detect the possible long-range order at  $T_{s2}$  because of technical reasons. Over the measured temperature range from 2 to 300 K, no clear anomaly signifying transitions is visible in  $C_p(T)$ . As shown in the insets



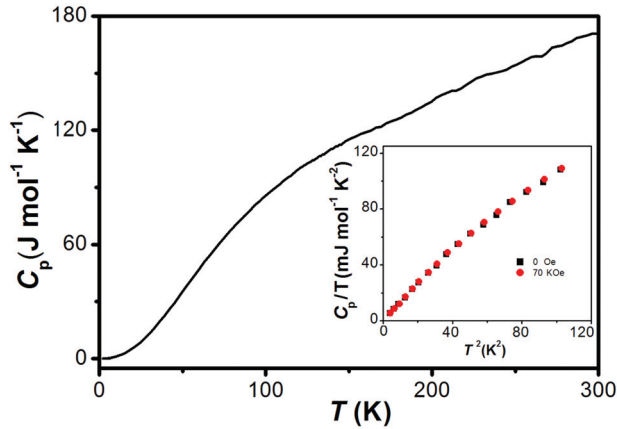


FIG. 5. (Color online) Temperature dependent heat capacity  $C_p$  of  $\text{Na}_2\text{Ti}_2\text{As}_2\text{O}$ . The inset shows the  $C_p/T$  vs  $T^2$  plot of the data measured in both 0- and 70-kOe magnetic fields.

in Fig. 3(a) and 3(b), the low-temperature portions of the data acquired from  $\text{Na}_2\text{Ti}_2\text{Sb}_2\text{O}$  and  $\text{Na}_2\text{Ti}_2\text{As}_2\text{O}$  below 20 K were preliminary analyzed using the approximated Debye model  $C_p/T = \gamma + 2.4\pi^4 r N_A k_B (1/T_D^3) T^2$ , where  $\gamma$  is a constant term,  $r$  is the number of atoms per formula unit,  $k_B$  is the Boltzmann constant, and  $T_D$  represents the Debye temperature. The analysis gave rise to a  $\gamma$  value of  $4.1 \text{ mJ mol}^{-1} \text{ K}^{-2}$  and a  $T_D$  of 239 K for  $\text{Na}_2\text{Ti}_2\text{Sb}_2\text{O}$ , as well as to a  $\gamma$  value of  $0 \text{ mJ mol}^{-1} \text{ K}^{-2}$  and a  $T_D$  of 218 K for  $\text{Na}_2\text{Ti}_2\text{As}_2\text{O}$ . These data indicate that finite densities of states are present at the Fermi level for  $\text{Na}_2\text{Ti}_2\text{Sb}_2\text{O}$  while  $\text{Na}_2\text{Ti}_2\text{As}_2\text{O}$  is fully gapped. In the presence of a magnetic field of 70 kOe, the results change slightly; values of  $\gamma$  of  $4.07 \text{ mJ mol}^{-1} \text{ K}^{-2}$  and  $0 \text{ mJ mol}^{-1} \text{ K}^{-2}$  for  $\text{Na}_2\text{Ti}_2\text{Sb}_2\text{O}$  and  $\text{Na}_2\text{Ti}_2\text{As}_2\text{O}$ , respectively, indicate small magnetic contributions to the low-temperature  $C_p(T)$ .

The present paper on single-crystal samples revealed remarkably strong electrical anisotropy for  $\text{Na}_2\text{Ti}_2\text{X}_2\text{O}$ . In particular, the  $\text{Na}_2\text{Ti}_2\text{As}_2\text{O}$  compound seems to possess multiple phase transitions and has more complex properties. Provided that the phase transitions in  $\text{Na}_2\text{Ti}_2\text{X}_2\text{O}$  are of the SDW type promoted by the nesting between electron and hole pockets, analogous to that in iron pnictides,<sup>9,10</sup> it would be of high possibility in producing exotic behaviors, including superconductivity through suppressing the SDW via carrier doping, or applying pressure, as did in iron pnictides.<sup>33-36</sup> Based on our present results, it is hard to distinguish the exact type of DW. Measurements using more sensitive

experimental probes on single crystals, like muon spin rotation or neutron diffraction, would hopefully give more in-depth insights. Moreover, the differences between  $\text{Na}_2\text{Ti}_2\text{Sb}_2\text{O}$  and  $\text{Na}_2\text{Ti}_2\text{As}_2\text{O}$ , including the different onset temperatures of phase transitions and electromagnetic behaviors, are possibly ascribed to the different energy levels of Sb and As  $p$  orbitals, because the only difference in their electronic structures is the hybridization states between the  $p$  orbitals of X and the  $3d$  orbitals of Ti.<sup>21,24</sup> Recalling that the SDW temperature of  $\text{LnFeAsO}$  is nearly robust to the change of rare earth elements Ln from La to Sm across a series of other Ln,<sup>37</sup> whereas it is more fragile to element replacement on an Fe or As site,<sup>33-35</sup> the different phase transition temperatures between  $\text{Na}_2\text{Ti}_2\text{Sb}_2\text{O}$  and  $\text{Na}_2\text{Ti}_2\text{As}_2\text{O}$  indicate the important role of X in  $\text{Na}_2\text{Ti}_2\text{X}_2\text{O}$  as that of Fe or As in iron arsenides.

#### IV. CONCLUSIONS

Electromagnetic characterizations on  $\text{Na}_2\text{Ti}_2\text{Sb}_2\text{O}$  and  $\text{Na}_2\text{Ti}_2\text{As}_2\text{O}$  crystals revealed remarkably strong anisotropy, with the electrical resistivity anisotropy with respect to  $H\parallel c$  and  $H\parallel ab$  directions even reaching the degrees of  $\sim 140$  and  $\sim 430$  for  $\text{Na}_2\text{Ti}_2\text{Sb}_2\text{O}$  and  $\text{Na}_2\text{Ti}_2\text{As}_2\text{O}$ , respectively, which are much higher than those for iron pnictides. Phase transition temperatures derived from the electromagnetic measurements coincide well with each other for  $\text{Na}_2\text{Ti}_2\text{Sb}_2\text{O}$  and  $\text{Na}_2\text{Ti}_2\text{As}_2\text{O}$ , respectively. The specific heat measurements revealed that  $\text{Na}_2\text{Ti}_2\text{Sb}_2\text{O}$  is partially gapped and  $\text{Na}_2\text{Ti}_2\text{As}_2\text{O}$  is fully gapped, and the phase transitions in them are likely less magnetic. However, as a possibly analogue to that in iron pnictides, the applied magnetic field of 70 kOe is too small to shift a DW anomaly. It needs a further check using higher magnetic fields. Unraveling the nature of the phase transition would be a crucial gradient toward understanding the unusual superconductivity, as well as to acquiring generic knowledge of the correlation between the superconductivity and a DW state in both layered titanium oxypnictide and iron pnictides. Study of this class of material thus supports continuous efforts.

#### ACKNOWLEDGMENTS

This paper was supported in part by the Ministry of Science and Technology of China (973 Projects No. 2011CB921701 and No. 2011CBA00110), National Natural Science Foundation of China (Grants No. 11274367 and No. 11120101003), and Chinese Academy of Sciences.

<sup>1</sup>T. Ito, H. Takagi, T. Ishibashi, and S. Uchida, *Nature* **350**, 596 (1991).

<sup>2</sup>K. Takenaka, K. Mizuhashi, H. Takagi, and S. Uchida, *Phys. Rev. B* **50**, 6534 (1994).

<sup>3</sup>D. N. Basov and T. Timusk, *Rev. Mod. Phys.* **77**, 721 (2005).

<sup>4</sup>A. Gozar, G. Logvenov, L. F. Kourkoutis, A. T. Bollinger, L. A. Giannuzzi, D. A. Muller, and I. Bozovic, *Nature (London)* **455**, 782 (2008).

<sup>5</sup>A. A. Schafgans, C. C. Homes, G. D. Gu, S. Komiya, Y. Ando, and D. N. Basov, *Phys. Rev. B* **82**, 100505(R) (2010).

<sup>6</sup>M. R. Norman, *Science* **332**, 196 (2011).

<sup>7</sup>R. M. Fleming, L. W. ter Haar, and F. J. DiSalvo, *Phys. Rev. B* **35**, 5388 (1987).

<sup>8</sup>E. Morosan, H. W. Zandbergen, B. S. Dennis, J. W. G. Bos, Y. Onose, T. Klimczuk, A. P. Ramirez, N. P. Ong, and R. J. Cava, *Nat. Phys.* **2**, 544 (2006).

<sup>9</sup>J. Dong, H. J. Zhang, G. Xu, Z. Li, G. Li, W. Z. Hu, D. Wu, G. F. Chen, X. Dai, J. L. Luo, Z. Fang, and N. L. Wang, *Europhys. Lett.* **83**, 27006 (2008).

<sup>10</sup>C. de la Cruz, Q. Huang, J. W. Lynn, J. Li, W. Ratcliff II, J. L. Zarestky, H. A. Mook, G. F. Chen, J. L. Luo, N. L. Wang, and P. C. Dai, *Nature (London)* **453**, 899 (2008).

- <sup>11</sup>J. G. Bednorz and K. A. Müller, *Z. Phys. B* **64**, 189 (1986).
- <sup>12</sup>I. I. Mazin, D. J. Singh, M. D. Johannes, and M. H. Du, *Phys. Rev. Lett.* **101**, 057003 (2008).
- <sup>13</sup>K. Kuroki, S. Onari, R. Arita, H. Usui, Y. Tanaka, H. Kontani, and H. Aoki, *Phys. Rev. Lett.* **101**, 087004 (2008).
- <sup>14</sup>V. Cvetkovic and Z. Tesanovic, *Europhys. Lett.* **85**, 37002 (2009).
- <sup>15</sup>E. A. Axtell III, T. Ozawa, S. M. Kauzlarich, and R. R. P. Singh, *J. Solid State Chem.* **134**, 423 (1997).
- <sup>16</sup>W. E. Pickett, *Phys. Rev. B* **58**, 4335 (1998).
- <sup>17</sup>T. C. Ozawa, S. M. Kauzlarich, M. Bieringer, and J. E. Greedan, *Chem. Mater.* **13**, 1804 (2001).
- <sup>18</sup>R. H. Liu, D. Tan, Y. A. Song, Q. J. Li, Y. J. Yan, J. J. Ying, Y. L. Xie, X. F. Wang, and X. H. Chen, *Phys. Rev. B* **80**, 144516 (2009).
- <sup>19</sup>X. F. Wang, Y. J. Yan, J. J. Ying, J. Q. Li, M. Zhang, N. Xu, and X. H. Chen, *J. Phys. Condens. Matter* **22**, 075702 (2010).
- <sup>20</sup>R. H. Liu, Y. A. Song, Q. J. Li, J. J. Ying, Y. J. Yan, Y. He, and X. H. Chen, *Chem. Mater.* **22**, 1503 (2010).
- <sup>21</sup>T. Yajima, K. Nakano, F. Takeiri, T. Ono, Y. Hosokoshi, Y. Matsushita, J. Heister, Y. Kobayashi, and H. Kageyama, *J. Phys. Soc. Jpn.* **81**, 103706 (2012).
- <sup>22</sup>P. Doan, M. Gooch, Z. Tang, B. Lorenz, A. Moeller, J. Tapp, P. C. W. Chu, and A. M. Guloy, *J. Am. Chem. Soc.* **134**, 16520 (2012).
- <sup>23</sup>H.-F. Zhai, W.-H. Jiao, Y.-L. Sun, J.-K. Bao, H. Jiang, X.-J. Yang, Z.-T. Tang, Q. Tao, X.-F. Xu, Y.-K. Li, C. Cao, J.-H. Dai, Z.-A. Xu, and G. H. Cao, *Phys. Rev. B* **87**, 100502(R) (2013).
- <sup>24</sup>T. Yajima, K. Nakano, F. Takeiri, J. Heister, T. Yamamoto, Y. Kobayashi, and H. Kageyama, *J. Phys. Soc. Jpn.* **82**, 013703 (2013).
- <sup>25</sup>T. C. Ozawa, T. Pantoja, E. A. Axtell III, S. M. Kauzlarich, J. E. Greedan, M. Bieringer, and J. W. Richardson, Jr., *J. Solid State Chem.* **153**, 275 (2000).
- <sup>26</sup>Y. Huang, H. P. Wang, W. D. Wang, Y. G. Shi, and N. L. Wang, *Phys. Rev. B* **87**, 100507(R) (2013).
- <sup>27</sup>A. Subedi, *Phys. Rev. B* **87**, 054506 (2013).
- <sup>28</sup>S. Kitagawa, K. Ishida, K. Nakano, T. Yajima, and H. Kageyama, *Phys. Rev. B* **87**, 060510(R) (2013).
- <sup>29</sup>H. Jiang, Y. L. Sun, J. H. Dai, G. H. Cao, and C. Cao, *arXiv:1207.6705*.
- <sup>30</sup>D. J. Singh, *New J. Phys.* **14**, 123003 (2012).
- <sup>31</sup>X. W. Yan and Z. Y. Lu, *J. Phys.: Condens. Matter* **25**, 365501 (2013).
- <sup>32</sup>H. C. Montgomery, *J. Appl. Phys.* **42**, 2971 (1971).
- <sup>33</sup>M. Rotter, M. Tegel, and D. Johrendt, *Phys. Rev. Lett.* **101**, 107006 (2008).
- <sup>34</sup>A. S. Sefat, R. Jin, M. A. McGuire, B. C. Sales, D. J. Singh, and D. Mandrus, *Phys. Rev. Lett.* **101**, 117004 (2008).
- <sup>35</sup>Z. Ren, Q. Tao, S. Jiang, C. M. Feng, C. Wang, J. H. Dai, G. H. Cao, and Z. A. Xu, *Phys. Rev. Lett.* **102**, 137002 (2009).
- <sup>36</sup>H. Okada, K. Igawa, H. Takahashi, Y. Kamihara, M. Hirano, H. Hosono, K. Matsubayashi, and Y. Uwatoko, *J. Phys. Soc. Jpn.* **77**, 113712 (2008).
- <sup>37</sup>K. Ishida, Y. Nakai, and H. Hosono, *J. Phys. Soc. Jpn.* **78**, 062001 (2009).